

# Comparison Radiography and Tomography Possibilities of FRM-II (20 MW) and Budapest (10 MW) Research Reactor

---

M. BALASKO<sup>1,\*</sup>, Ä. KUBA<sup>2</sup>, A. TANÁCS<sup>2</sup>, Z. KISS<sup>2</sup>, A. NAGY<sup>2</sup>  
and B. SCHILLINGER<sup>3</sup>

**Abstract.** In November of 2005 a measurement series was conducted on different kinds of reference objects to compare the results of the FRM-II (ANTARES) and the Budapest (Radiography Station) research reactor in the field of neutron radiography, gamma radiography, classical tomography and discrete tomography by an ANDOR CCD camera and Imaging plate with BAS 2500 Scanner (contributed by AIDA software).

## INTRODUCTION

The Radiography Station began to work in the spring of 1994 in Budapest and the ANTARES radiography working place began to work on the spring of 2004 in Garching. Interesting possibility to compare the capabilities of the two stations by different imaging techniques with complemented radiations on some practical investigated objects, as a VAILLANT type streaming pump, made from complex materials, a gas pressure regulator, made from aluminum casting, and three pieces radiator valves are in one group, made from grass.

In additional we have investigated the gas pressure regulator with classical and discrete tomography. The preprocessing methods and the tomographic procedures also will be presented in the paper.

## 1. EXPERIMENTAL FACILITY

The ANTARES began to work on the spring of 2004 in Garching [1]. The Radiography Station (RS) began to work on the spring of 1994 in Budapest [2],[3]. We summarized the main parameters of the both station briefly in the Table 1.

<sup>1</sup>MTA KFKI Atomic Energy Research Institute, H-1525 Budapest POBox 49.,Hungary

<sup>2</sup>University of Szeged, Dept. of Image Processing and Computer Graphics, H-6720 Szeged, Hungary

<sup>3</sup>FRM-II and Faculty for Physics E21, Technische Universität München, Garching, Germany

\*Corresponding author E-mail: balasko@sunserv.kfki.hu

**Table 1.** Summarized parameters.

Parameter	Dimension	FRM-II reactor ANTARES	Budapest reactor Radiography Station
Neutron flux	$n\text{ cm}^{-2}\text{ sec}^{-1}$	$9,4 \times 10^7$	$8 \times 10^7$
Collimator ratio (L/D)		400 (800)	200
Cd ratio		15	8
Gamma dose rate	Sv/h	0.69 (0.17)	8.3
Area of the exposure field	mm	300 X 400	Diameter 225
Detector		ANDOR CCD camera	Imaging Plate
Resolution	pixel	2048 X 2048	5000 X 4000
Dynamics	bit	16	16
Tomography methods		Classical	Classical and discrete
Projection of tomography	Step	200 or 400	20
Applied software		OCTOPUS, house made	SNARK 94 and house made
Mechanical loading	kg	500	300

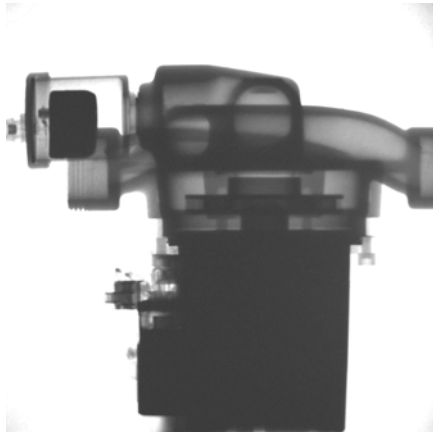
## 2. INVESTIGATED OBJECTS

The applied reference objects were the following: a VAILLANT type streaming pump, made from various materials; a gas pressure regulator made from aluminum casting; and a three piece radiator valve made from brass.

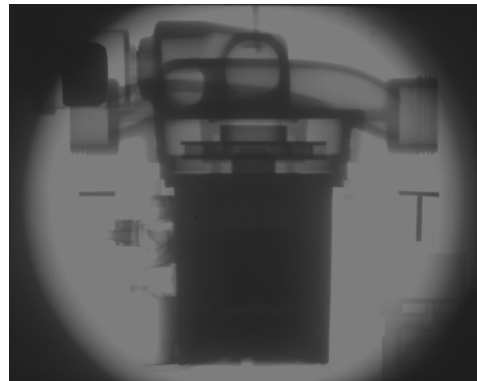
## 3. MEASUREMENTS

### 3.1. VAILLANT Type Circulation Pump

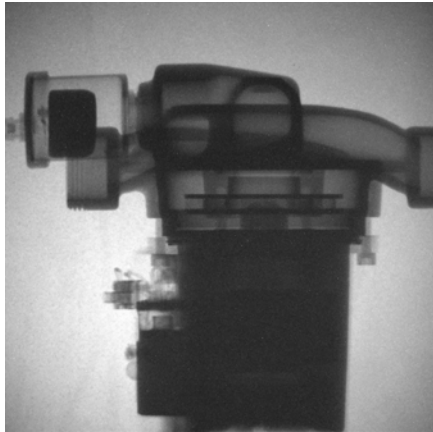
The VAILLANT type circulation pump consists of an electric driver motor which is isolated by artificial resin in its housing and the radial-flow pump housing (made from steel) with a turbine. The series of different kinds of radiography pictures (Figure 1, Figure 2, and Figure 3) shows the characteristic properties of low energy-, thermal-, and epithermal neutron and gamma radiation.



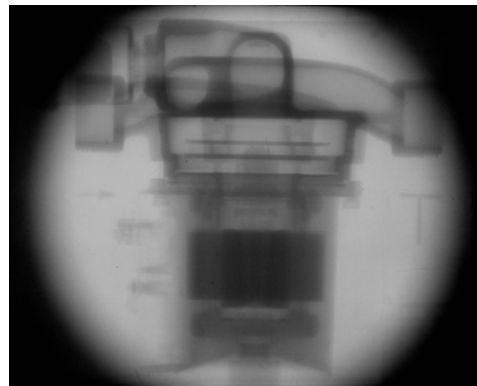
a.) ANTARES by CCD camera



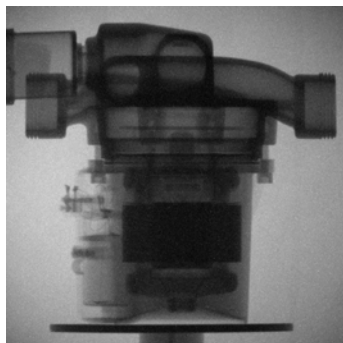
b.) RS by IP

**FIGURE 1.** NR picture of the Vaillant pump.

a.) ANTARES by CCD camera



b.) RS by IP

**FIGURE 2.** ENR picture of the Vaillant pump.

a.) ANTARES by CCD camera



b.) the RS by IP

**FIGURE 3.** GR picture of the Vaillant pump.

A survey of the exposure conditions is in Table 2.

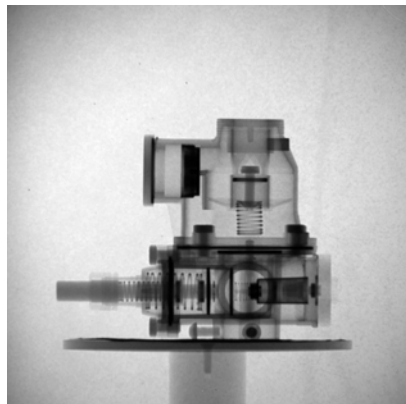
**Table 2.** Exposure conditions.

Figure	Applied radiation	Filtering	Exposure time	Notice
1.a	Low energy neutron	NO	6 sec	
1.b	Thermal neutron	100mm Pb	60 sec	
2.a	Epithermal neutron	2 mm Cd	360 sec	
2.b	Epithermal neutron	100 mm Pb+2mm Cd	900 sec	
3.a	Reactor gamma	10 mm B <sub>4</sub> C	120 sec	
3.b	Reactor gamma	50 mm Pb	15 sec	

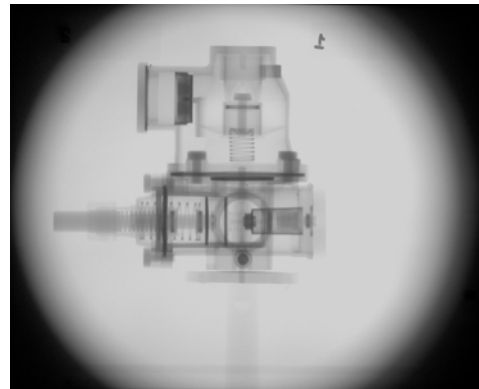
The sharpness of the all pictures is better on the ANTARES due to its higher collimator ratio. The two different radiation compositions of the two beams gave different shadings of the pictures. On the NR picture the low energy neutrons of ANTARES shows many details of the small thickness of impregnating artificial resin in Figure 1.a. The penetration of the thermal neutrons is better, and they are able to give information about the distribution of the impregnating artificial resin in Figure 1.b. The two epithermal NR (ENR) pictures (see Figure 2) are easily distinguishable. The ENR picture of ANTARES is similar to the thermal NR picture, while the ENR of RS Budapest is rather similar to the GR picture. The intensity of the gamma radiation is high at the Budapest reactor and the GR picture (see Figure 3.b) of RS contains more details than the GR picture (see Figure 3.a) of ANTARES.

### 3.2. Gas Pressure Regulator

The housing of the gas pressure regulator is made from aluminum casting. Its inner structure is very complex as it is visible in Figure 4. It contains of wide range of the different materials, as sealings from gum, sensor from brash, springs from phosphorus-bronze and the screws from iron.



a.) ANTARES by CCD camera



b.) RS by IP

**FIGURE 4.** NR picture of the gas pressure regulator.

### 3.3. Radiator Valves

The radiator valves are made from brass, and the material of the sealing was gum. The upper and the middle valves are closed state while the lower is open as in both Figure 5.a and Figure 5.b. The exposure time was 6 s on the ANTARES, and 90 s on RS. The upper valves contain some limescales as it is shown in Figure 6 by a tomography slice of ANTARES's reconstruction. The limescales were lost during the transport from FMR-II to Budapest unfortunately, as is visible in Figure 5.b.

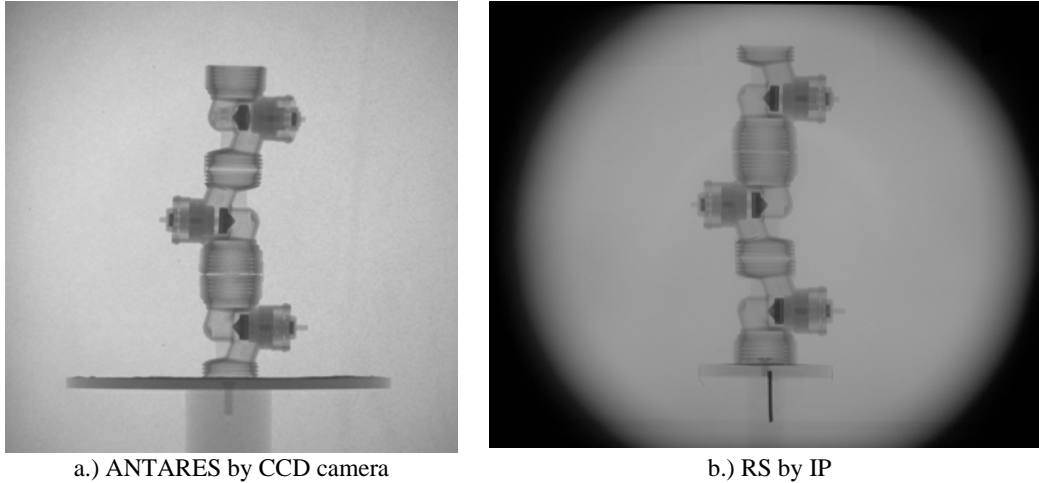


*FIGURE 5. NR picture of radiator valves.*

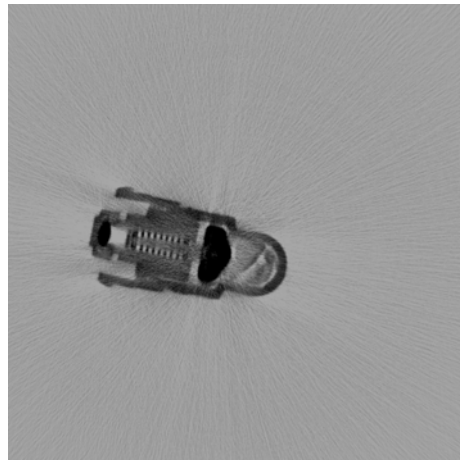


*FIGURE 6. Limescales in the upper radiator valve.*

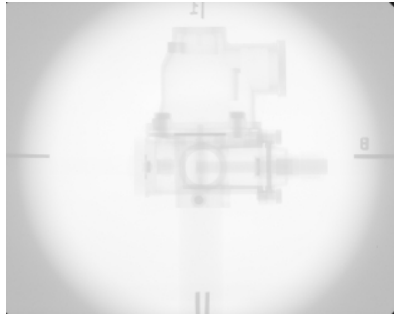
## 4. NEUTRON TOMOGRAPHY

Before the reconstruction we corrected the projections in order to get a better reconstruction result. These corrections were performed on the ANTARES and Radiography Station data on-demand. We have applied classical Filtered Back

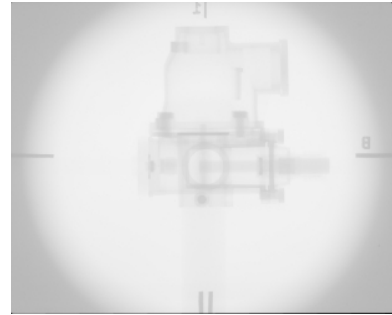
Projection (FBP) and Discrete Tomography (DT) methods on the gas pressure regulator measured data. The results are presented in this section

#### 4.1. Projection Correction Methods

The correction methods will be presented on the Radiography Station measurements. The Radiography Station projections were acquired by an imaging plate detector. This detector was shifted and rotated during the measurement (see Figure 7.a).



7a. unregistered projection



7b. registered projection

**FIGURE 7.** *The unregistered and registered projections.*

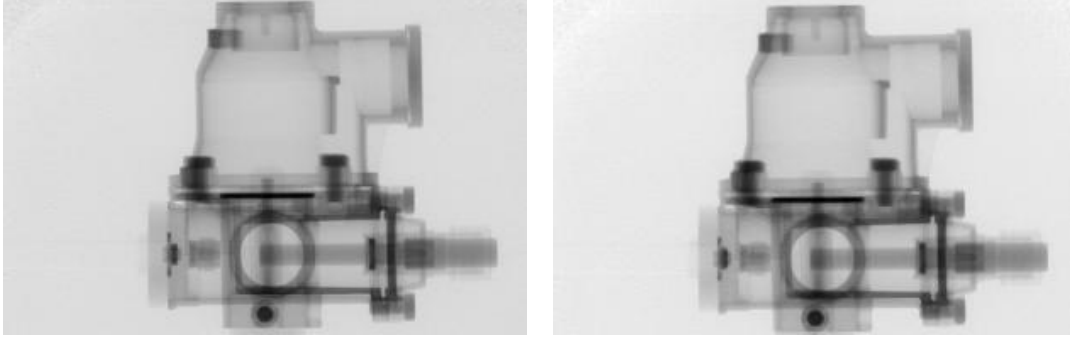
The way the images are taken introduces geometric differences between the consecutive projections. It means that the same projection directions from the source might pass the imaging plate at different pixel locations. Such geometric differences can degrade the result of the reconstruction. An image registration algorithm is applied to recover these geometric differences.

It is assumed that a rigid-body transformation (translation along the axis and rotation about the center of the image) can align the images. Our previously developed automatic registration algorithm utilizes the normalized version of mutual information such as pixel similarity measure [4]. Although the algorithm is fully automatic, a preprocessing step is necessary. The center region of the images, where the projection of the object is visible must be masked out and the similarity measure is evaluated only outside of it. To eliminate the rotational invariance, artificial markers are affixed in front of the imaging plate, the projections of which are visible in the top, bottom, left and right hand side of the images. One of the projection images is selected as the reference image and the others, including the open beam projection image, are registered against it one by one. Visual inspection confirmed that the registration provided acceptable results (see Figure 7.b).

We have cropped the area which contains the objects in all projections. We did not want to reconstruct the empty area. After cropping the relevant part of the projection we have resampled the projections in order to reduce the reconstruction time for DT.

The projections produced by neutron rays have distortions. Some of these distortions come from the image acquisition system itself. In order to reduce the effects of these

we have to correct them. To correcting the uniformity distortion we need the open beam projection. For each projection we have to multiply all pixels with the corresponding open beam projection reciprocal value (see Figure 8.a). If the projection intensity is changing during the measurement, we have to correct it in such way that the average intensity should be constant in the background area (see Figure 8.b).



8a. Uniformity

8b. Intensity

**FIGURE 8.** Projections after uniformity correction.

After these preprocessing methods we have to find the initial beam energy to perform a logarithmic transform. We have taken the average mean of the projections where there is no object to be found. This method gives a good approximation if we do not know the value exactly.

The Classical Filtered Back Projection method is the most general reconstruction algorithm. Further details can be found on this topic in [6].

In the case of the discrete tomography method, the reconstruction problem is equivalent to finding a solution of the linear equation system

$$Ax = b, \text{ where } x \in D = \{0, K, d_n\}. \quad (1)$$

The  $A$  matrix can be calculated knowing the geometry of the acquisition system. If we do not have so many projections then the number of equations is less than the number of unknowns. This means that it can have several solutions, even discrete number valued ones. Furthermore, due to the measurement errors, we are looking for the solution which is close to the exact one. According this we can reformulate the solution of the equation system to the optimization problem in the following way:

$$C(x) = \|Ax - b\|^2 + \gamma \cdot \Phi(x), \quad (2)$$

where the first term controls that  $x$  is satisfying the (eq. 1) approximately. The second terms allows us to include a prior information  $x$  into the optimization problem. In our case, e tried to find such kind of  $x$  which has large coherent regions.

$$\Phi(x) = \sum_{j=0}^m \sum_{l \in Q_j^k} g_{l,j} |\xi_j - \xi_l|, \quad (3)$$

where in  $Q$  environment of the current position we penalize the first term of the (eq. 2) with the difference and the distance between the two positions.

Since we are looking for a discrete-valued  $x$ , the numerical optimization methods are not suitable here. We have chosen the Simulated Annealing (SA) optimization procedure [5].

#### 4.2. Neutron Tomography at ANTARES

We have applied the classical FBP method on the ANTARES measurement after the correction methods were performed. Due to the huge number of projection we have quite good reconstruction results. Furthermore, we can observe some distortions on both slices which probably means these come from scattering and beam hardening (see Figure9).

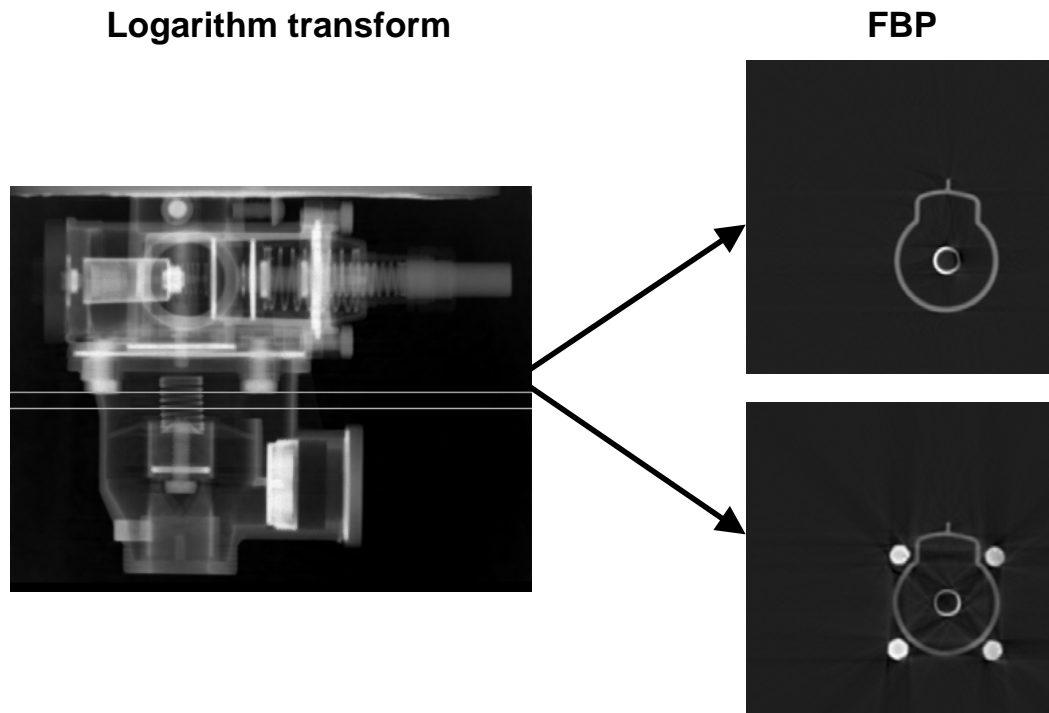


**FIGURE 9.** Result of the classical FBP method on ANTARES (400 projections).

#### 4.3. Neutron Tomography at Radiography Station

We have removed the inner part of the gas pressure regulator in order to have binary valued slices. We have tried to determine the attenuation coefficient for these slices by performing reconstruction with different attenuation values. This heuristic method took account the first term value of the (eq. 2) objective function and the value of the smoothness (eq. 3) of the reconstructed object. After that we moved a type of slice which contains more then two value inside and we tried to find the next attenuation coefficient. The result for two and three valued slices can be seen in Figure0. The result of three valued slice has some errors which come from other projection

distortions that can be seen on the classical FBP results in addition to the fact that this slices actually not three valued but four valued.

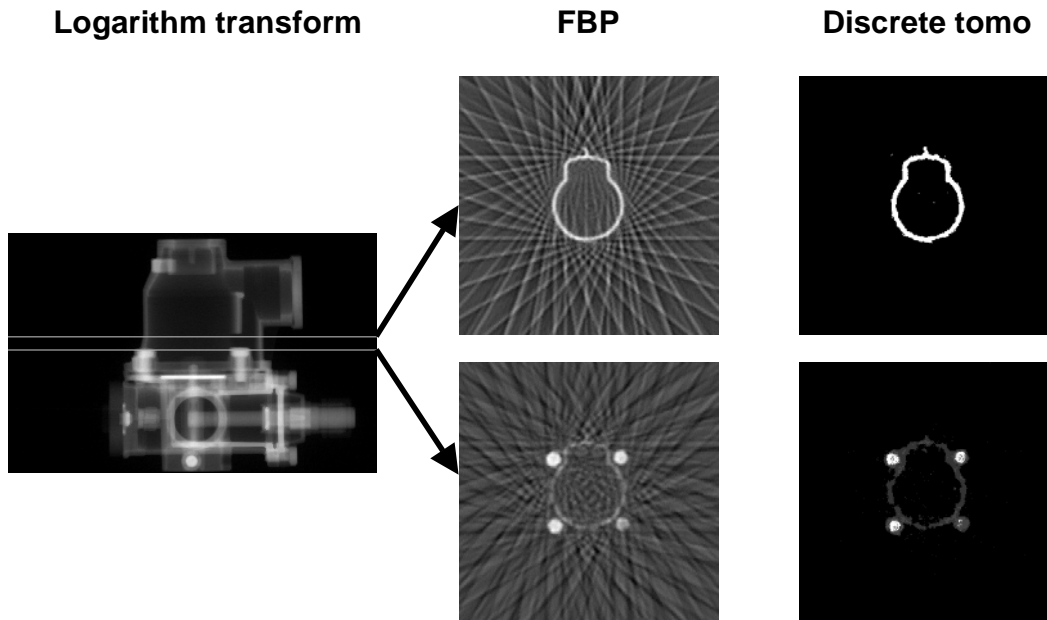


*FIGURE 10. Results of the classical FBP and DT method on Radiography Station (18 projections).*

## CONCLUSIONS

Evidently, the sharpness of the all pictures is better on the ANTARES due to its higher collimator ratio. The two different radiation compositions of the two beams give different shadings of the pictures. The NR pictures of the low energy neutrons of ANTARES show many details of the objects, but the penetration of the thermal neutrons of RS Budapest is better in the hydrogen containing material. The ENR picture of ANTARES is similar to the low energy NR picture of it, while the ENR of RS Budapest is rather similar to the GR picture of it. The intensity of the gamma radiation is high at the Budapest reactor and its GR picture contains more details then the GR picture of ANTARES.

According to the reconstruction results we can establish that correcting the projections is necessary to get better results. These correction methods tend to get uniform normalized projections. Furthermore in special cases we have to register the projections to each other in order to correct the imaging plate displacements after the acquisition. Other correction methods are needed which take into account other distortions of the projections (e.g. scattering, beam hardening). Two kinds of reconstruction methods were applied on the corrected projection data. The classical filtered back projection gives good results at a high number of projections. Naturally we get better results if we have larger numbers of projections in the case of the classical reconstruction method. The discrete tomography method can be applied when the object consists of two materials and the number of projections is low. Further

investigation in the future is necessary for cases when the object consists of three or more materials.

## ACKNOWLEDGMENTS

This work was supported by OTKA T048476 grant.

## REFERENCES

- [1] E. Calzada, B. Schillinger and F. Grünauer, *Construction and assembly of neutron radiography and tomography facility ANTARES at FRM-II*, Nuclear Instruments and Methods in Physics Research A 542 (2005) 38–45.
- [2] M. Balaskó, E. Sváb, *Dynamic neutron radiography instrumentation and applications*, Central Europe, Nuclear Instruments and Methods in Physics Research A 377, 140–143 (1996)
- [3] Márton Balaskó, Attila Kuba, Antal Nagy, Zoltán Kiss, Lajos Rodek, László Ruskó *Neutron-, gamma-, and X-ray three-dimensional computed tomography at the Budapest research reactor site*, Nuclear Instruments and Methods in Physics Research A 542 (2005) 22–27
- [4] Attila Tanács, Attila Kuba: *Evaluation of a Fully Automatic Medical Image Registration Algorithm Based on Mutual Information*, Acta Cybernetica 16 (2003) 327–336
- [5] N. Metropolis, A. Rosenbluth, M. Rosenbluth, A. Teller, and E. Teller *Equation of state calculation by fast computing machines*, J. Chem. Phys. 21 (1953)
- [6] A. C. Kak and M. Slaney. *Principles of Computerized Tomographic Imaging*. IEEE Press, Inc., New York, 1988.